eXPRESS Polymer Letters Vol.14, No.3 (2020) 235–247
Available online at www.expresspolymlett.com
https://doi.org/10.3144/expresspolymlett.2020.20

Dually-functional riboflavin macromolecule as a supramolecular initiator and reducing agent in temporally-controlled low ppm ATRP

*I. Zaborniak, P. Chmielarz**

Department of Physical Chemistry, Faculty of Chemistry, Rzeszów University of Technology, Al. Powstańców Warszawy 6, 35-959 Rzeszów, Poland

Received 15 June 2019; accepted in revised form 19 August 2019

Abstract. A novel supramolecular riboflavin-inspired macroinitiator was prepared for the first time by transesterification methodology and used as the multifunctional vitamin-B_2 core to synthesize PBA brushes using different low ppm atom transfer radical polymerization (ATRP) approaches. Firstly the macromolecular initiator was successfully applied as a dually-functional structure, which simultaneously acts as a reducing agent in activator regeneration by electron transfer (ARGET) ATRP. Subsequently simplified electrochemically mediated ATRP of BA with different conditions was carried out for the preparation of well-defined riboflavin-based polymer brushes. Polymerizations were characterized in a well-controlled manner, affording polymers with a narrow dispersity ($Đ$ = 1.22–1.25). Four-arms polymers were also received by an approach never described before – temporally-controlled multi-step *se*ATRP under constant current conditions, giving precisely-defined polymer brushes ($Đ$ = 1.26) with preserved chain-end functionality (DCF < 1%), despite stopping and restarting the polymerization. The solvolysis results indicate that all chains grow to equal lengths ($Đ$ < 1.17), which shows the precisely controlled characteristic of *se*ATRP. ^{1}H NMR analysis confirms the formation of new vitamin B_2-inspired polymers. In connection with the preserved riboflavin functionality and additional functional chains, these innovative macromolecules may find applications, *e.g.* as drug delivery systems.

Keywords: *polymer synthesis, dually-functional riboflavin macromolecule, temporally-controlled multi-step current electrolysis, seATRP, vitamin B_2-inspired polymer brushes*

1. Introduction

Synthesis of functional polymeric materials by modification of naturally-derived substrates, in particular with unique properties, recently attracts increasing attention [1–4]. Considering a wide range of different monomers with various functionalities, incorporation into an appropriate polymer chain improves existing properties in the biomolecule or provides completely novel features. An interesting biological molecule constituting an excellent substrate to prepare new types of polymers with different characteristics is riboflavin (vitamin B_2) [5, 6]. It is a water-soluble vitamin present in a wide range of food products, *e.g.* milk, dairy products, meat, fish, and also dark-green vegetables [7–9]. Vitamin B_2 is composed of two essential components – isoalloxazine ring and ribitol side chain containing four hydroxyl groups [10]. The first part is characteristic for flavin family and is responsible for the occurrence of redox processes. This behavior is closely related to the key role of riboflavin, more precisely of its biologically active forms – flavin adenine dinucleotide (FAD) and flavin mononucleotide (FMN), in the energy metabolism of some primary metabolites (fats, carbohydrates, proteins and ketone bodies) [11–15]. Meanwhile, the second structural component creates the

*Corresponding author, e-mail: p_chmiel@prz.edu.pl

potential possibility to the efficient incorporation of brominated atom transfer radical polymerization (ATRP) initiation sites due to the presence of hydroxyl groups. The uniqueness of ATRP in the frame of conventional radical polymerization results from a few essential advantages including narrow molecular weight distribution (MWD, M_w/M_n, $Đ$) and control over molecular weight (MW) of the prepared, precisely designed macromolecules, and also the possibility to site-specific incorporation of functionalities [16–21]. In this context, the crucial predominance of ATRP solution is the opportunity to control polymer topology and obtain various structures, ranging from linear chains [22], brushes [23], cycles [24], stars [25], combs [26], up to regular networks [27]. The most representative ATRP approaches use low loadings of catalyst complex due to additional redox cycle causing continuous regeneration of activators. These methods take advantage of various chemical reducing agents (*e.g.* glucose [28] and ascorbic acid [29]) in activators regenerated by electron transfer (ARGET) technique or zerovalent metals (*e.g.* Cu^0 and Fe^0) as supplemental activators and mild reducing agents (SARA) [30–32], and interestingly as external stimuli, as a reducing current in electrochemically mediated ATRP (*e*ATRP) [19, 33–35] and its type – simplified electrochemically mediated ATRP (*se*ATRP) [36–39]. The use of electrochemistry eliminates chemical reducing agents [40], creates an opportunity to recycle the catalyst [41] and temporal control by stopping and restarting the polymerization, simultaneously maintaining control during the process [20, 42]. From both industrial and experimental points of view, an attractive approach in the context of *se*ATRP is electrolysis under galvanostatic conditions [43]. The unquestionable advantage of this method is providing a constant current and eliminating a reference electrode (RE) from the reaction setup [44].

One of the versatile ATRP synthetic approaches is undoubtedly grafting-from solution. The procedure includes two main steps: (1) preparation of a functional macroinitiator by the direct incorporation brominated initiation sites instead of hydroxyl groups, followed by (2) the polymerization of monomer to prepare graft (co)polymer [25, 32, 45, 46].

This article presents a synthesis of a novel ATRP macroinitiator based on the naturally-derived substrate – riboflavin and its application in ATRP in two different contextscontexts (Figure 2). Firstly, it was successfully applied as the dually-functional riboflavin-inspired macroinitiator which simultaneously acts as a reducing agent due to the presence of an unmodified isoalloxazine ring responsible for redox processes of the riboflavin part of the molecule. The next objective of this paper is to show the use of the multifunctional macroinitiator in the synthesis of precisely controlled polymers, consisting of riboflavin core and poly(butyl acrylate) (PBA) side chains *via* presented for the first time – temporally-controlled *se*ATRP under galvanostatic condition. Prepared macromolecules – besides unique riboflavin properties resulting from preservation of the characteristic isoalloxazine ring –are characterized by hydrophobic properties due to PBA side chains incorporation, providing an efficient substrate to prepare polymer materials with decreased wettability [47] with potential application as polymer coatings with precisely designed surface polarity [48–50].

2. Experimental section

2.1. Materials

Riboflavin (Rib, M_n = 376.36, 98%), 2-bromoisobutyryl bromide (BriBBr, 98%), *N*-methyl-2-pyrrolidone (NMP, >99%), dichloromethane (DCM, >99.9%), magnesium sulfate ($MgSO_4$, >99.5%), tetrahydrofuran (THF, >99.9%), methanol (MeOH, >99.8%), tetrabutylammonium perchlorate (TBAP, >98%), copper(II) bromide ($Cu^{II}Br_2$, 99.9%) were purchased from Aldrich. *N*,*N*-Dimethylformamide (DMF, 99.9%) was purchased from Acros. These reagents were used without further purification. Tris(2-pyridylmethyl)amine (TPMA) was prepared according to a published procedure [51], $Cu^{II}Br_2$/TPMA catalyst complex was prepared as previously reported [36]. Before use, butyl acrylate (BA, > 99% Aldrich) was passed through a column filled with basic alumina to remove inhibitor. Pt gauze (99.9% metals basis), Al wire, Pt mesh and Pt disk (3 mm diameter, Gamry) were purchased from Alfa Aesar. Cyclic voltammetry (CV) and electrolysis were carried out in a five-neck electrochemical cell.

2.2. Analysis

^1H NMR spectra in DMSO-d_6 and $CDCl_3$ were measured with a Bruker Avance 500 MHz spectrometer. Monomer conversion and theoretical number-average molecular weight ($M_{n,th}$) were determined from NMR analysis [37]. MWs and MWDs were received from Viscotek T60A GPC (guard, 10^5, 10^3, and 10^2 Å

PSS columns; THF as eluent, flow rate 1.00 ml/min, PS calibration).

CV was performed using an Autolab model AUT84337 potentiostat running with a GPES software. The working electrode (WE), RE and counter electrode (CE) was a platinum disk (0.071 cm^2), saturated calomel electrode (SCE) and an Al wire (l = 10 cm, d = 1 mm), respectively.

Electrolyses under potentiostatic and galvanostatic conditions were recorded on a Metrohm Autolab potentiostat using a platinum mesh (A = ~6 cm^2) as WE and Al wire (l = 10 cm, d = 1 mm) as CE. During polymerization the temperature was kept at 50 °C using a circulating thermostat (Labo Play ESM-3711-H). Values for applied potential during electrolysis were obtained from CV measurements (0.1 V/s) with SCE as RE.

2.3. Synthesis of the riboflavin-based ATRP macroinitiator (Rib-Br_4)

The synthetic route for the preparation of the riboflavin-based macromolecule ATRP initiator is shown in Figure 1. Riboflavin (0.25 g, 0.66 mmol) was dissolved in NMP (6 ml) under Ar atmosphere in a 25 ml round bottom flask. A solution of BriBBr (0.98 ml, 7.97 mmol) in NMP (2 ml) was added dropwise for 0.5 h at 0 °C; then the reaction solution was stirred for 7 days at room temperature. Upon completion, the product was diluted with dichloromethane (20 ml) and washed with water (100 ml × 15), dried ($MgSO_4$), filtered and concentrated under reduced pressure. The resulting orange solid product was dried under vacuum (0.33 g, yield 52%). The resulting product was characterized using GPC and ^{1}H NMR.

2.4. Riboflavin ARGET ATRP in preparation of Rib-*g*-(PBA-Br)$_4$ graft polymers

9.9 ml of BA (69.2 mmol), DMF (8.80 ml) and 280 µl of $Cu^{II}Br_2$/TPMA stock solution (0.05 M in DMF) were added to the Ar purged two-neck round bottom flask (25 ml) at 50 °C. Next, a solution of 112 mg of Rib-Br_4 (0.12 mmol) in 1 ml of DMF was injected. Samples were withdrawn periodically to kinetics investigation by ^{1}H NMR analysis. The polymerization was stopped after 214 h by opening the flask and exposing the catalyst to air. The M_n and M_w/M_n were established by GPC measurements. Before GPC the samples were dissolved in THF, passed through a neutral alumina column, dried under vacuum for 1 day, dissolved in methanol, and finally precipitated in water. The final product was characterized by ^{1}H NMR and GPC after isolation and purification.

2.5. Synthesis of Rib-*g*-(PBA-Br)$_4$ graft polymers *via se*ATRP with a constant potential

The synthesis of Rib-*g*-(PBA-Br)$_4$ polymer was conducted *via* preparative electrolysis under constant potential conditions (Figure 7a). The Pt mesh WE, Al wire CE, and SCE RE were prepared and located in the polymerization cell. 1.37 g of TBAP (4.0 mmol), 9.92 ml of BA (69.2 mmol), 8.80 ml of DMF and 280 µl of $Cu^{II}Br_2$/TPMA stock solution (0.05 M in DMF) were introduced into the cell at 50 °C under a slow Ar purge. Then, 112 mg of Rib-Br_4 (0.12 mmol) in 1 ml of DMF was added. Before the electrolysis, a CV curve was recorded to determine the appropriately potential (E_{app} = –0.276 V; Figure 6) using during *se*ATRP. Samples were withdrawn periodically to kinetics investigation by

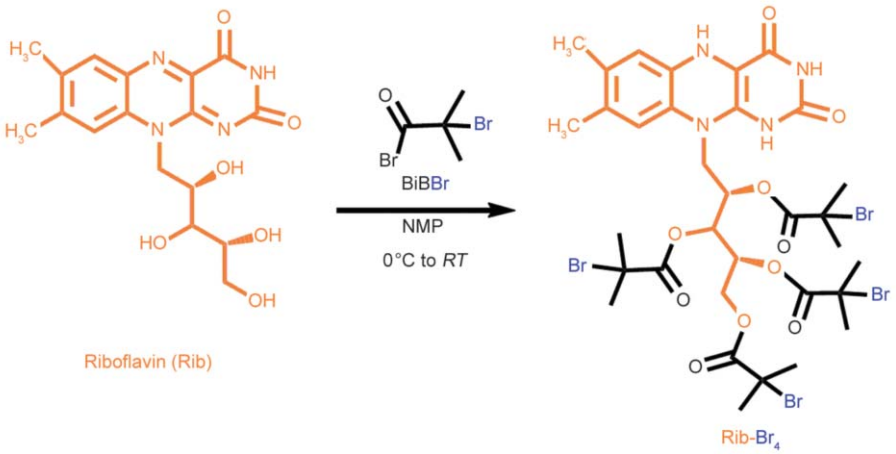

Figure 1. Synthetic route for the preparation of the brominated riboflavin macromolecule.

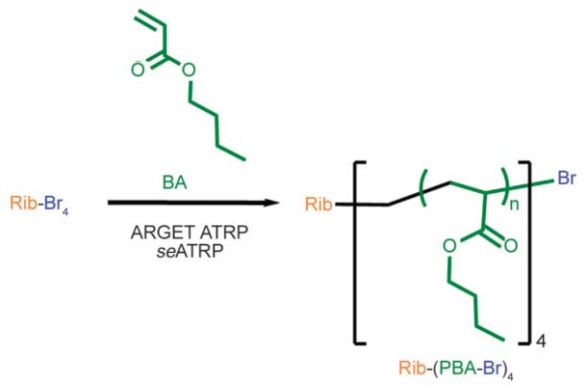

Figure 2. Preparation of Rib-*g*-(PBA-Br)$_4$ graft polymers *via* ARGET ATRP with dually-functional ATRP macroinitiator or *se*ATRP under potentiostatic and temporally-controlled galvanostatic conditions.

^{1}H NMR analysis. The M_n and M_w/M_n were established by GPC measurements. Before GPC the samples were dissolved in THF, passed through a neutral alumina column, dried under vacuum for 1 day, dissolved in methanol, and finally precipitated in water. The final product was characterized by ^{1}H NMR and GPC after isolation and purification.

2.6. Synthesis of Rib-*g*-(PBA-Br)$_4$ graft polymers *via* temporally-controlled *se*ATRP under galvanostatic conditions

*se*ATRP with periodically applied different values of current (I_{app} = –1.38, –0.95, –0.73, –0.55, –0.44 and –0.58 mA for ON stages and I_{app} = 0 mA for OFF stages) was used (Figure 7e). 1.37 g of TBAP (4.0 mmol), 9.92 ml of BA (69.2 mmol), 8.80 ml of DMF and 280 µl of $Cu^{II}Br_2$/TPMA stock solution (0.05 M in DMF) were introduced into the cell at 50 °C under a slow Ar purge. Then, 112 mg of Rib-Br$_4$ (0.12 mmol) in 1 ml of DMF was added. An appropriate current value for each ON stage was calculated on the basis of $I = Q/s$, taking into account previously conducted constant potential electrolysis, whereas OFF stages were characterized by the current value of zero. Samples were withdrawn periodically to kinetics investigation by ^{1}H NMR analysis. The M_n and M_w/M_n were established by GPC measurements. Before GPC the samples were dissolved in THF, passed through a neutral alumina column, dried under vacuum for 1 day, dissolved in methanol, and finally precipitated in water. The final product was characterized by ^{1}H NMR and GPC after isolation and purification.

2.7. Synthesis of Rib-*g*-(PBA-Br)$_4$ graft polymers *via* accelerated *se*ATRP with constant applied potential

The synthesis of Rib-*g*-(PBA-Br)$_4$ polymer was conducted *via* accelerated preparative electrolysis under constant potential conditions (Figure 9a). The Pt mesh WE, Al wire CE, and SCE RE were prepared and located in the polymerization cell. 0.68 g of TBAP (2.0 mmol), 4.0 ml of BA (27.9 mmol), 4.78 ml of DMF and 223 µl of $Cu^{II}Br_2$/TPMA stock solution (0.05 M in DMF) were introduced into the cell at 50 °C under a slow Ar purge. Then, 61.7 mg of Rib-Br$_4$ (0.06 mmol) in 1 ml of DMF was added. Before the electrolysis, a CV was recorded to determine the appropriate potential (E_{app} = –0.301 V; Figure 8) using during *se*ATRP. Samples were withdrawn periodically to kinetics investigation by ^{1}H NMR analysis. The M_n and M_w/M_n were established by GPC measurements. Before GPC the samples were dissolved in THF, passed through a neutral alumina column, dried under vacuum for 1 day, dissolved in methanol, and finally precipitated in water. The final product was characterized by ^{1}H NMR and GPC after isolation and purification.

2.8. Analysis of Rib-(PBA-Br)$_4$ polymer chains

The analysis of the chain length of the polymer brushes was conducted by cleaving the PBA chains attached to the riboflavin core by acid solvolysis according to the procedure described in reference [39]. The resulting polymers were analyzed by GPC, determining apparent M_n and $Đ$ of PBA chains.

3. Results and discussion

A riboflavin-inspired macromolecular initiator with 4 brominated initiation sites (Rib-Br$_4$) was prepared for the first time using synthetic route based on transesterification reaction of riboflavin with BriBBr in NMP as a solvent (Figure 1, M_n = 972, $Đ$ = 1.27). The chemical structure of Rib-Br$_4$ was confirmed by ^{1}H NMR (Figure 3): δ [ppm] = 1.85–2.01 (28H, C*H*$_3$–, **a**), 2.38–2.40 (3H, C*H*$_3$–, **b**), 2.46–2.48 (3H, C*H*$_3$–, **c**), 4.32–5.15 (4H, –C*H*–, –C*H*$_2$–, –C*H*–, **d**), 5.63–5.71 (1H, –C*H*–, **e**), 5.71–5.83 (2H, –C*H*$_2$–, **f+g**), 7.67–7.77 (1H, =C*H*–, **h**), 7.87–7.93 (1H, =C*H*–, **i**), 11.36–11.44 (1H, N*H*–, **j**), and 13.04–13.55 (2H, N*H*–, **k**, oxidized form of riboflavin) [6, 52,

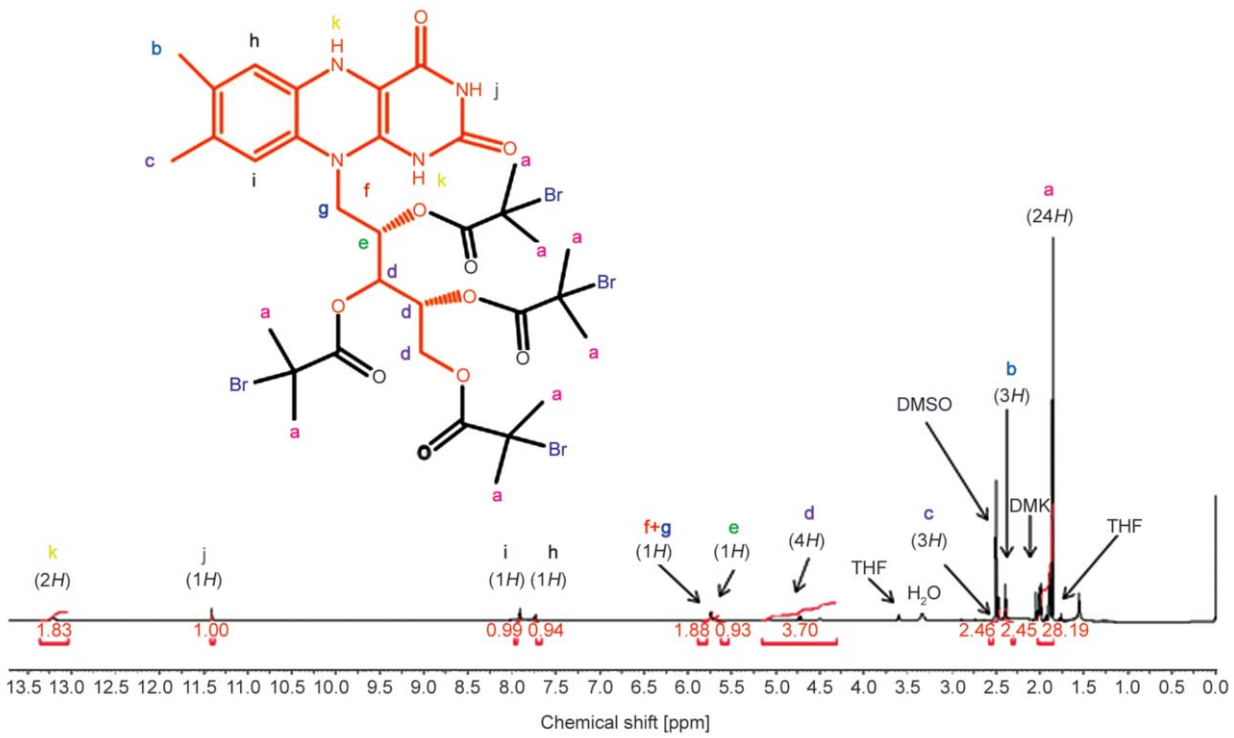

Figure 3. ^{1}H NMR analysis of Rib-Br$_4$ supramolecular initiator (in DMSO-d_6).

53]. The degree of substitution of the hydroxyl groups of the ribitol side chain of riboflavin was determined by the ratio between the areas of the amine proton at the regions of δ = 11.36–11.44 ppm (1H) and the methyl groups protons of the incorporated bromide structure at the region of δ = 1.85–2.01 ppm (28H). The result of this analysis shows the riboflavin-based product has 4 Br functionalities.

The synthesized multifunctional macroinitiator constitutes a substrate to the synthesis of completely new riboflavin-inspired polymer brushes with PBA side chains using low ppm ATRP methods. The first objective includes a new sight for ARGET ATRP methods due to using Rib-Br$_4$ as a dually-functional molecule acts simultaneously as a macroinitiator and a reducing agent, resulting in the successful synthesis of vitamin-based macromolecules (Figure 4, Table 1, entry 1). The more efficient and controlled approach in the preparation of functional riboflavin-derived polymers using received macroinitiator proved to be the electrochemically controlled living polymerization, more precisely electrolysis under constant potential condition and reported for the first time, more industrially relevant – temporally-controlled *se*ATRP under galvanostatic condition (Figure 4, Table 1, entries 2–4).

3.1. ARGET ATRP with dually-functional riboflavin-inspired macroinitiator in preparation of Rib-*g*-(PBA-Br)$_4$ macromolecules

A completely innovative ARGET ATRP approach was used in preparation of novel vitamin B$_2$-based polymers. The uniqueness of this solution relies on the use of the dually-functional molecule, which is simultaneously an initiator – due to the presence of brominated initiation sites incorporated into ribitol side chain, and efficient reducing agent – in connection with preserved redox functional isoalloxazine ring of the riboflavin core. Considering the reducing agent functionality of the riboflavin-based structure, it efficiently reduced Cu^{II} to Cu^{I}, which is evidenced by successfully received macromolecules confirmed by GPC analysis (Figure 5b). First-order kinetics plot (Figure 5a) indicates constant concertation of propagating radicals during polymerization, however lack of linearity between M_w/M_n and monomer conversion (Figure 5b), and broad molecular weight distribution of final polymer (Figure 5a, Table 1, entry 1) show loose of control manner of the polymerization process. This phenomenon is associated with a relatively high molar excess of reducing agent to deactivator (17 eqiv.) resulting in fast reduction of the whole Cu^{II} to Cu^{I} and the presence of mere activator in the reaction system.

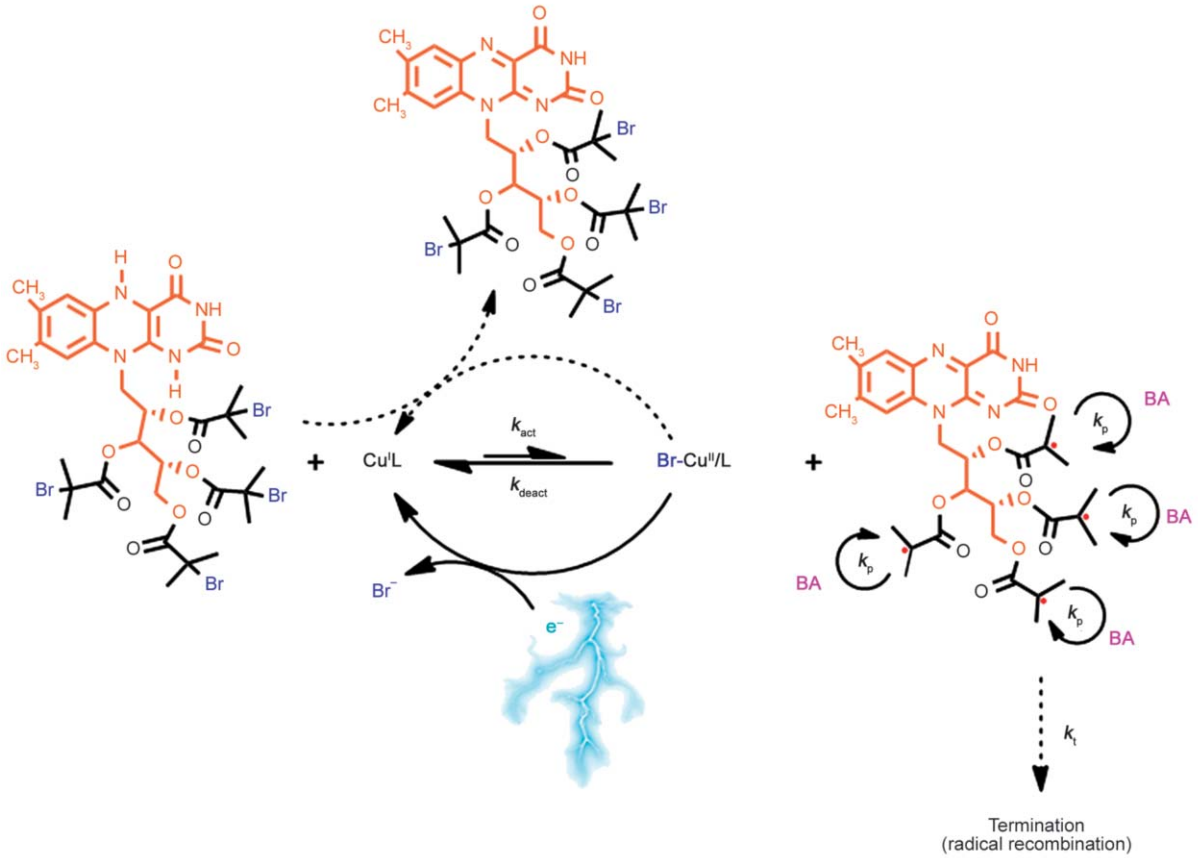

Figure 4. Mechanism of ATRP process with regeneration of activators by electric current and oxidation of dually-functional riboflavin-inspired macroinitiators. Solid arrows represent the main mechanism of reduction of deactivators, dashed arrows – supplemental mechanism.

Table 1. Summary of riboflavin-inspired macromolecules synthesis.

Entry	$[BA]_0/[Rib\text{-}Br_4]_0/[Cu^{II}Br_2]_0/[TPMA]_0$	E_{app} [a]	k_p^{app} [b] [h^{-1}]	$M_{n,th}$ [c] ($\cdot 10^{-3}$)	$DP_{n,th}$ [b] (chain)	$M_{n,app}$ [d] ($\cdot 10^{-3}$)	$DP_{n,app}$ [e] (chain)	M_w/M_n [d]	DCF [f] [%]
1	150/1/0.03/0.06	–	0.0014	19.1	37	13.2	24	1.94	0.00
2	150/1/0.03/0.06	E_{pc} – 70 mV	0.0760	25.4	48	17.6	34	1.25	0.02
3	150/1/0.03/0.06	Temporally-controlled I_{app} electrolysis [g]	0.0910 [h]	25.4	48	18.1	36	1.26	0.03
4	110/1/0.04/0.09	E_{pc} – 90 mV	0.1340	39.9	76	37.6	72	1.22	0.10

General reaction conditions:
T = 50 °C; V_{tot} = 16 ml (except entry 4: V_{tot} = 10 ml);
t = 5 h (except entry 1: t = 214 h and entry 4: t = 10 h;
for entry 3: ON stages = 5 h, OFF stages = 1.5 h);
$[BA]_0$ = 3.5 M (except entry 4: $[BA]_0$ = 2);
$[Rib\text{-}Br_4]_0$ = 5.8 mM calculated per 4 Br initiation sites (except entry 4: $[Rib\text{-}Br_4]_0$ = 6.3 mM calculated per 4 Br initiation sites);
$[Cu^{II}Br_2/TPMA]$ = 0.7 mM (except entry 4: $[Cu^{II}Br_2/TPMA]_0$ = 1.1 mM);
ARGET ATRP with dually-functional riboflavin-based ATRP macroinitiator: entry 1;
Constant potential *se*ATRP (WE = Pt, CE = Al, RE = SCE): entry 2 and 4;
*se*ATRP under temporally-controlled galvanostatic conditions (WE and CE without RE): entry 3.
[a] E_{app} were selected based on CV analysis of $Cu^{II}Br_2$/TPMA catalytic complexes (Figure 6 and 8);
[b] Apparent rate constant of propagation (k_p^{app}) and apparent theoretical degree of polymerization of monomer unit per arm ($DP_{n,theo}$) were determined by NMR [20];
[c] $M_{n,th} = ([BA]_0/[Rib\text{-}Br_4]_0)\cdot conversion\cdot M_{BA} + M_{Rib\text{-}Br_4}$;
[d] apparent M_n and M_w/M_n were determined by GPC;
[e] $DP_{n,app}$ (per chain) = $M_{n,app}$ (per chain)/M_{BA} [51];
[f] Estimated according to reference [55];
[g] I_{app} = –1.38, –0.95, –0.73, –0.55, –0.44 and –0.58 mA for each steps;
[h] Only for the 'ON' stages.

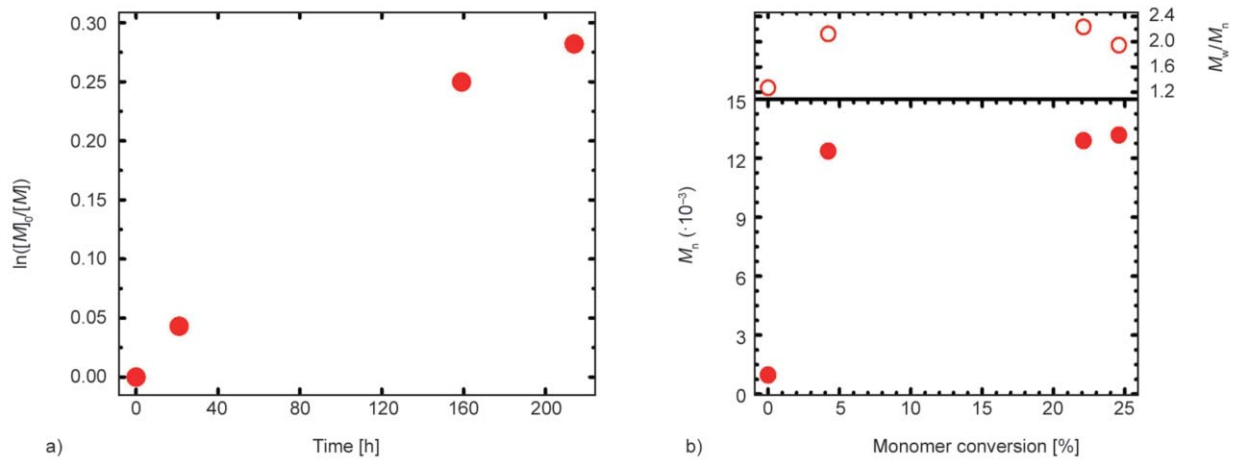

Figure 5. (a) First-order kinetic plot of monomer conversion *vs.* polymerization time, and (b) M_n and M_w/M_n *vs.* monomer conversion by ARGET ATRP. Table 1, entry 1.

Despite reducing agent characteristic, the naturally-derived supramolecule proves to be simultaneously an effective initiator in the polymerization of BA forming side chains of the riboflavin-based macroinitiator. The received polymeric products were clearly evidenced by GPC analysis (Figure 5b, Table 1, entry 1).

3.2. Synthesis of multi-branched chain Rib-*g*-(PBA-Br)$_4$ macromolecules *via se*ATRP under constant potential and temporally-controlled constant current electrolysis conditions

Electrochemistry, as an efficient external stimulus in the continuous reduction of Cu^{II} in the view of ATRP techniques, has been applied for the first time to prepare functional riboflavin-based polymer brushes with PBA side chains. The homopolymer macromolecular brushes with 4 side arms of PBA was synthesized using constant potential conditions and multiple-step galvanostatic electrolysis (Figure 7a, Table 1, entry 2 and 3, respectively). Considering constant potential solution, current profile *vs.* polymerization time at the initial step of polymerization indicates presence merely deactivator, however along with the polymerization process, an effective electrochemical reduction of the deactivator to the activator occurs in the system, what is reflected by the cathodic current decay, finally resulting in constant ratio of deactivator/activator corresponding to the current value, established by the selected E_{app} (Figure 6, Table 1, entry 2).

A linear first-order kinetic plot (Figure 7b) and low M_w/M_n values (Figure 7c) were observed, indicating a well-controlled ATRP process. This controlled

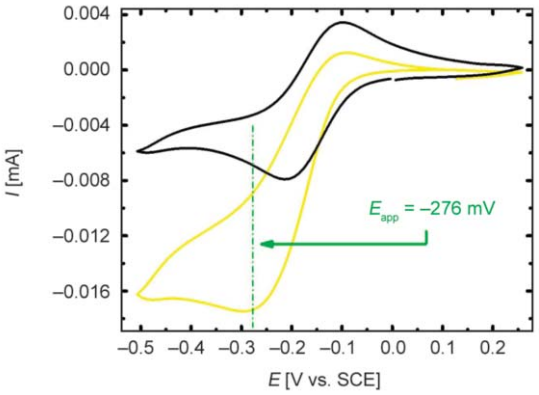

Figure 6. Cyclic voltammogram of 0.7 mM $Cu^{II}Br_2$/TPMA in 50% (v/v) BA/DMF ([BA] = 3.5 M) containing 0.2 M TBAP in the absence (black line) and in the presence of 5.8 mM of Rib-Br_4 (yellow line) recorded at $v = 0.1$ V·s^{-1}.

manner of polymerization was also clearly proved by GPC traces (Figure 7d) of samples withdrawn periodically during synthesis, demonstrating the continuous evolution of the molecular weight during the whole process.

Bearing in mind the industrial and experimental benefits, an attractive approach in the context of *se*ATRP is highly simplified electrolysis under constant current conditions due to removing a reference electrode from reaction setup and a possibility to use simple current generator compared with the electrolysis under potentiostatic mode [38, 43, 44, 56]. This approach was applied in the synthesis of riboflavin-based macromolecular brushes with 4 side arms of PBA. Moreover, it was improved by introducing temporal control during polymerization, verifying at the same time the living nature of the electrochemically mediated process and allowing the preparation of polymer brush chains with predictable molecular

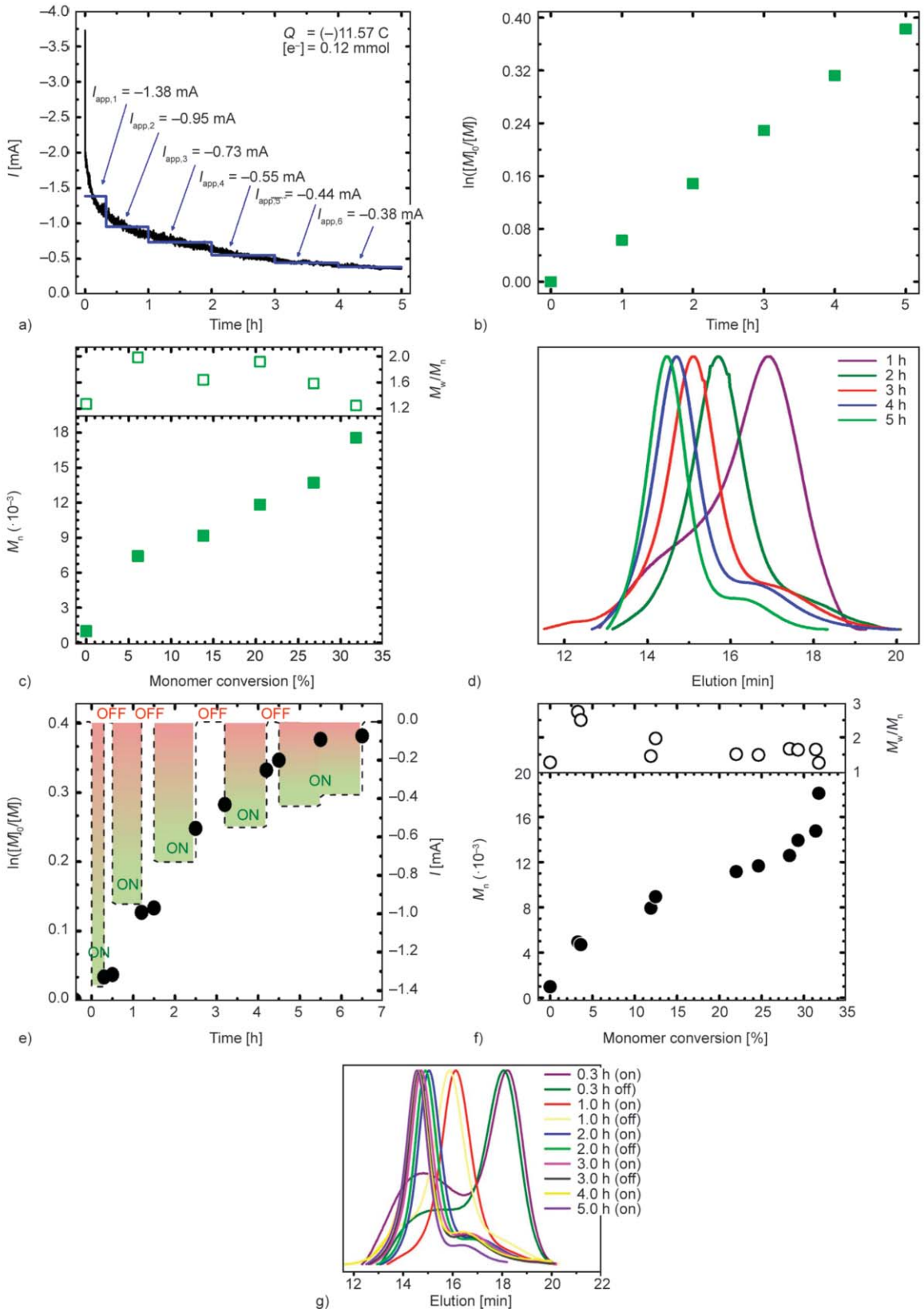

Figure 7. Synthesis of Rib-(PBA-Br)$_4$ macromolecules through *se*ATRP under constant potential conditions: (a) current profile *vs.* polymerization time; (b) first-order kinetic plot of monomer conversion *vs.* polymerization time, (c) M_n and M_w/M_n *vs.* monomer conversion; (d) GPC traces of BA polymerization and their evolution over reaction time. Table 1, entry 2. Synthesis of Rib-(PBA-Br)$_4$ macromolecules under temporally-controlled galvanostatic conditions: (e) first-order kinetic plot of *se*ATRP using few different step by applied appropriate current *i.e.* I_{app} = –1.38, –0.95, –0.73, –0.55, –0.44 and –0.58 mA for each steps, respectively; (f) M_n and M_w/M_n *vs.* monomer conversion; (g) GPC traces of BA polymerization and their evolution over reaction time. Table 1, entry 3.

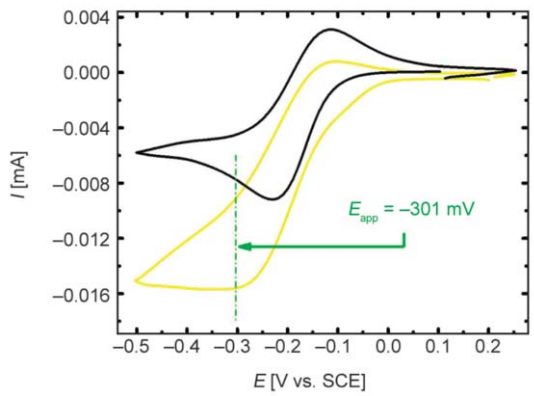

Figure 8. Cyclic voltammogram of 1.1 mM $Cu^{II}Br_2$/TPMA in 40% (v/v) BA/DMF ([BA] = 2.8 M) containing 0.2 M TBAP in the absence (black line) and in the presence of 6.3 mM of Rib-Br_4 (yellow line) recorded at $v = 0.1$ V·s^{-1}.

weights. It was demonstrated by a 10 step constant current preparative electrolysis including 6 ON stages characterized by an appropriate current value calculated on the basis of $I = Q/s$, taking into account previously conducted constant potential electrolysis, and 4 OFF stages – the current instantaneously drops to zero (Figure 7a and 7e, Table 1, entry 3). The observed trend of M_n *vs.* monomer conversion and the evolution of GPC traces of BA over time (Figure 7g) confirms the livingness of the polymerization (Figure 7f). The DCF value (below 1%) denoting the % of chains terminated by radical disproportionation, indicates that even though the stopping and restarting the polymerization, the chains continued to grow each time after triggered the polymerization with preserving chain end functionality. Thus, under appropriate selected electrolysis conditions, the proportion of terminated chains could be sufficiently small (typically below 1 mol%) that it does not interfere with the designed architecture [41, 57].

To synthesize well-defined high molecular weight brush-like macromolecules, optimized reaction setup through higher catalyst loading and more negative E_{app} (Figure 8) during the polymerization was applied. As expected, in this case also the typical behavior of constant potential *e*ATRP was observed, what means,

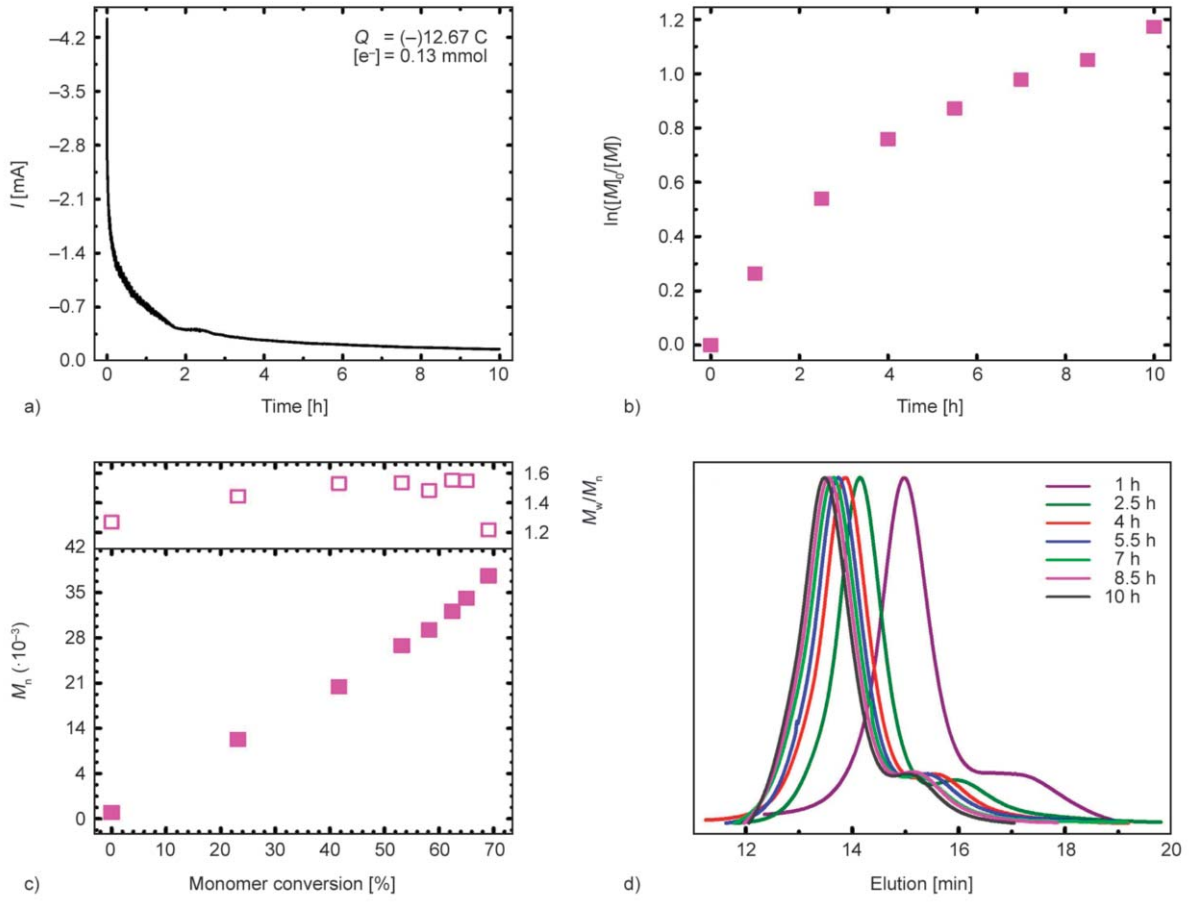

Figure 9. Synthesis of Rib-*g*-(PBA-Br)$_4$ macromolecules through *se*ATRP under constant potential conditions: (a) current profile *vs.* polymerization time; (b) first-order kinetic plot of monomer conversion *vs.* polymerization time, (c) M_n and M_w/M_n *vs.* monomer conversion; (d) GPC traces of BA polymerization and their evolution over time. Table 1, entry 4.

the cathodic current rapidly decays at the beginning of polymerization due to starting the conversion of Cu^{II} to Cu^{I} species, up to achieve thermodynamic equilibrium (Figure 9a). This approach allows receiving high molecular weight polymer brushes in a controlled manner proved by linear first-order kinetics plot (Figure 9b) and molecular weight evolution (Figure 9c). Furthermore, GPC traces showing a clean shift in the molecular weight peak toward higher M_n were registered (Figure 9d).

Comparing the two low ppm ATRP solutions (ARGET ATRP *vs. se*ATRP), the results indicate electrochemical approaches as an efficient reducing force for well-controlled ATRP. Moreover, it proves the advantage of the electrochemical reduction mechanism of the deactivator over dually-functionality of applied macroinitiator in ARGET ATRP, while eliminating the effects of its reducing agent characteristic, and thus providing polymers with narrow molecular weight distributions ($Đ$ = 1.22).

The ^{1}H NMR analysis confirms the structure of the Rib-(PBA-Br)$_4$ brush-like polymer obtained through *se*ATRP under potentiostatic conditions (Table 1, entry 4): δ [ppm] = 0.69–1.06 (3H, C*H*$_3$–), 1.28–1.43 (2H, –C*H*$_2$–CH$_3$), 1.52–1.82 (2H, –CH$_2$–C*H*$_2$–CH$_2$–), 1.87–2.03 (2H, –C*H*$_2$–C*H*<), 2.20–2.47 (1H, –C*H*<), and 3.85–4.25 (1H, –OC*H*$_2$–) [37, 39, 58]. The identified chemical shifts are mainly attributed to the –CH$_3$, –CH$_2$–, –CH–, and –OCH$_2$– groups of the PBA units in the arms, respectively, indicating the presence of PBA chains.

3.3. Analysis of the PBA chains length cleaved from brush-like polymer

To confirm the well-controlled manner of electrochemically-mediated polymerization processes and unambiguously determine the number of the chain of received polymer brushes, the chains were cleaved from macromolecules by acid solvolysis, and therefore the apparent molecular weights of cleaved chains and initiation efficiency (f_i) were established (Table 2).

The results of solvolysis demonstrate precise control during polymerization processes indicating homopolymer side chains characterized by low molecular weight and low dispersity ($Đ$ < 1.19), what points out that all chains grow simultaneously to equal lengths during the syntheses. Moreover, apparent MW of analyzed PBA chains closely followed theoretical MW, affecting in high initiation efficiency of received macromolecules, especially in the case of temporally-controlled electrolysis under galvanostatic conditions (f_i) (Table 2, entry 3), showing this method once again as an attractive and efficient approach form the both experimental and industrial point of view. Following the solvolysis results, especially high apparent and theoretical MW conformity, the quadruple initiation functionality of brominated riboflavin was clearly confirmed.

4. Conclusions

The novel vitamin B$_2$-inspired polymer brushes were successfully synthesized by two-step synthetic route. The first stage includes preparation of the ATRP macroinitiator by transesterification reaction of α-bromoisobutyryl bromide with riboflavin constituting dually-functional supramolecular structure due to preserving redox-responsive isoalloxazine ring of riboflavin and incorporation of functional polymers into the ribitol chains. The second step concerns the first report of applying of ATRP methods with diminished catalyst concentration for the receiving well-defined polymer brushes based on riboflavin molecule. The dual functionality – as an initiator and a reducing agent – of the supramolecular structure was implemented in ARGET ATRP, providing four-arms macromolecules. Precisely-controlled polymeric brushes ($Đ$ = 1.22–1.25) were obtained using

Table 2. Results of the PBA chains analysis cleaved from the riboflavin-based macromolecules.

Entry (according to Table 1)	$M_{n,theo}$[(a)] (·10^{-3}) (chain)	$DP_{n,theo}$[(b)] (chain)	$M_{n,app}$[(c)] (·10^{-3}) (chain)	$DP_{n,app}$[(b)] (chain)	M_w/M_n[(c)]	f_i[(d)] [%]
2	6.2	48	8.8	69	1.19	70
3	6.2	48	6.1	48	1.17	100
4	9.7	76	17.3	135	1.06	56

[(a)] $M_{n,th}$ = ([BA]$_0$/[Rib-Br$_4$]$_0$)·conversion·M_{BA}, where [BA]$_0$ and [Rib-Br$_4$]$_0$ are the initial monomer and initiation site concentrations, respectively;

[(b)] established according to Table 1;

[(c)] apparent M_n and M_w/M_n of the arms cleaved from the riboflavin-inspired brushes executed by THF GPC (PS standards);

[(d)] efficiency of initiation: f_i = ($DP_{n,theo}$ (per chain)/$DP_{n,app}$ (per chain))·100%.

preparative electrolysis under constant potential electrolysis. This approach allows receiving high molecular weight polymer brushes in a controlled manner proved by linear first-order kinetics plot and molecular weight evolution. Furthermore, this paper describes for the first time highly industrial applicable approach – temporally-controlled simplified electrolysis under constant current conditions. The use of a galvanostatic mode with stopping and restarting of the process provided similar results to polymerizations conducted under potentiostatic conditions, providing polymers with molecular weight evolution close to theoretical values, while generating brushes with preserved chain-end functionality and narrow molecular weight distribution ($Đ = 1.26$). The solvolysis results confirm the precisely controlled manner of the electrochemically mediated process in both potentiostatic and galvanostatic conditions, receiving low molecular weight PBA homopolymers with low dispersity ($Đ < 1.17$) and high conformity of apparent and theoretical MW. The results from ^{1}H NMR analyses support the formation of PBA polymer brushes. These novel riboflavin-inspired polymers as precursors of polyelectrolyte are promising materials for applying in a wide range of medical branches, such as drug delivery.

Acknowledgements

Financial support from DS.CF.18.001, DS./M.CF.18.002, DS./M.CF.18.005 is gratefully acknowledged. P.C. acknowledges Minister of Science and Higher Education scholarship for outstanding young scientists (0001/E-363/STYP/13/2018). NMR spectra were recorded in the Laboratory of Spectrometry, Faculty of Chemistry, Rzeszow University of Technology and were financed from budget of statutory activities.

References

[1] Carlini A. S., Adamiak L., Gianneschi N. C.: Biosynthetic polymers as functional materials. Macromolecules, **49**, 4379–4394 (2016). https://doi.org/10.1021/acs.macromol.6b00439

[2] Celikkin N., Rinoldi C., Costantini M., Trombetta M., Rainer A., Święszkowski W.: Naturally derived proteins and glycosaminoglycan scaffolds for tissue engineering applications. Materials Science and Engineering: C, **78**, 1277–1299 (2017). https://doi.org/10.1016/j.msec.2017.04.016

[3] Xiong R., Grant A. M., Ma R., Zhang S., Tsukruk V. V.: Naturally-derived biopolymer nanocomposites: Interfacial design, properties and emerging applications. Materials Science and Engineering: R: Reports, **125**, 1–41 (2018). https://doi.org/10.1016/j.mser.2018.01.002

[4] Austin M. J., Rosales A. M.: Tunable biomaterials from synthetic, sequence-controlled polymers. Biomaterials Science, **7**, 490–505 (2019). https://doi.org/10.1039/C8BM01215F

[5] Iida H., Iwahana S., Mizoguchi T., Yashima E.: Main-chain optically active riboflavin polymer for asymmetric catalysis and its vapochromic behavior. Journal of the American Chemical Society, **134**, 15103–15113 (2012). https://doi.org/10.1021/ja306159t

[6] Metternich J. B., Sagebiel S., Lückener A., Lamping S., Ravoo B. J., Gilmour R.: Covalent immobilization of (−)-riboflavin on polymer functionalized silica particles: Application in the photocatalytic E→Z isomerization of polarized alkenes. Chemistry – A European Journal, **24**, 4228–4233 (2018). https://doi.org/10.1002/chem.201800231

[7] Powers H. J.: Riboflavin (vitamin B-2) and health. The American Journal of Clinical Nutrition, **77**, 1352–1360 (2003). https://doi.org/10.1093/ajcn/77.6.1352

[8] Nohr D., Biesalski H. K.: Vitamins in milk and dairy products: B-group vitamins. in 'Advanced dairy chemistry: Volume 3: Lactose, water, salts and minor constituents' (eds.: McSweeney P., Fox P. F.) Springer, New York, Vol 3, 591–630 (2009).

[9] Amin F., Khan W., Bano B.: Oxidation of cystatin imparted by riboflavin generated free radicals: Spectral analysis. International Journal of Biological Macromolecules, **124**, 1281–1291 (2019). https://doi.org/10.1016/j.ijbiomac.2018.12.021

[10] Pinto J. T., Zempleni J.: Riboflavin. Advances in Nutrition, **7**, 973–975 (2016). https://doi.org/10.3945/an.116.012716

[11] Yamashita M., Rosatto S. S., Kubota L. T.: Electrochemical comparative study of riboflavin, FMN and FAD immobilized on the silica gel modified with zirconium oxide. Journal of the Brazilian Chemical Society, **13**, 635–641 (2002). https://doi.org/10.1590/S0103-50532002000500015

[12] Abbas C. A., Sibirny A. A.: Genetic control of biosynthesis and transport of riboflavin and flavin nucleotides and construction of robust biotechnological producers. Microbiology and Molecular Biology Reviews, **75**, 321–360 (2011). https://doi.org/10.1128/mmbr.00030-10

[13] Northrop-Clewes C. A., Thurnham D. I.: The discovery and characterization of riboflavin. Annals of Nutrition and Metabolism, **61**, 224–230 (2012). https://doi.org/10.1159/000343111

[14] Kim S., Kim C. M., Son Y-J., Choi J. Y., Siegenthaler R. K., Lee Y., Jang T-H., Song J., Kang H., Kaiser C. A., Park H. H.: Molecular basis of maintaining an oxidizing environment under anaerobiosis by soluble fumarate reductase. Nature Communications, **9**, 4867/1–4867/12 (2018). https://doi.org/10.1038/s41467-018-07285-9

[15] Rostas A., Einholz C., Illarionov B., Heidinger L., Said T. A., Bauss A., Fischer M., Bacher A., Weber S., Schleicher E.: Long-lived hydrated FMN radicals: EPR characterization and implications for catalytic variability in flavoproteins. Journal of the American Chemical Society, **140**, 16521–16527 (2018). https://doi.org/10.1021/jacs.8b07544

[16] Wang J-S., Matyjaszewski K.: Controlled/'living' radical polymerization. Atom transfer radical polymerization in the presence of transition-metal complexes. Journal of the American Chemical Society, **117**, 5614–5615 (1995). https://doi.org/10.1021/ja00125a035

[17] Matyjaszewski K., Tsarevsky N. V.: Nanostructured functional materials prepared by atom transfer radical polymerization. Nature Chemistry, **1**, 276–288 (2009). https://doi.org/10.1038/nchem.257

[18] Boyer C., Corrigan N. A., Jung K., Nguyen D., Nguyen T-K., Adnan N. N. M., Oliver S., Shanmugam S., Yeow J.: Copper-mediated living radical polymerization (atom transfer radical polymerization and copper(0) mediated polymerization): From fundamentals to bioapplications. Chemical Reviews, **116**, 1803–1949 (2016). https://doi.org/10.1021/acs.chemrev.5b00396

[19] Chmielarz P., Fantin M., Park S., Isse A. A., Gennaro A., Magenau A. J. D., Sobkowiak A., Matyjaszewski K.: Electrochemically mediated atom transfer radical polymerization (*e*ATRP). Progress in Polymer Science, **69**, 47–78 (2017). https://doi.org/10.1016/j.progpolymsci.2017.02.005

[20] Chmielarz P., Pacześniak T., Rydel-Ciszek K., Zaborniak I., Biedka P., Sobkowiak A.: Synthesis of naturally-derived macromolecules through simplified electrochemically mediated ATRP. Beilstein Journal of Organic Chemistry, **13**, 2466–2472 (2017). https://doi.org/10.3762/bjoc.13.243

[21] Yan J., Malakooti M. H., Lu Z., Wang Z., Kazem N., Pan C., Bockstaller M. R., Majidi C., Matyjaszewski K.: Solution processable liquid metal nanodroplets by surface-initiated atom transfer radical polymerization. Nature Nanotechnology, **14**, 684–690 (2019). https://doi.org/10.1038/s41565-019-0454-6

[22] Fantin M., Isse A. A., Venzo A., Gennaro A., Matyjaszewski K.: Atom transfer radical polymerization of methacrylic acid: A won challenge. Journal of the American Chemical Society, **138**, 7216–7219 (2016). https://doi.org/10.1021/jacs.6b01935

[23] Jiang L., Messing M., Ye L.: Temperature and PH dual-responsive core-brush nanocomposite for enrichment of glycoproteins. ACS Applied Materials and Interfaces, **9**, 8985–8995 (2017). https://doi.org/10.1021/acsami.6b15326

[24] Nicolaÿ R., Matyjaszewski K.: Synthesis of cyclic (*co*)-polymers by atom transfer radical cross-coupling and ring expansion by nitroxide-mediated polymerization. Macromolecules, **44**, 240–247 (2011). https://doi.org/10.1021/ma102313q

[25] Chmielarz P.: Synthesis of cationic star polymers by simplified electrochemically mediated ATRP. Express Polymer Letters, **10**, 810–821 (2016). https://doi.org/10.3144/expresspolymlett.2016.76

[26] Wang Z. H., Li W. B., Ma J., Tang G. P., Yang W. T., Xu F. J.: Functionalized nonionic dextran backbones by atom transfer radical polymerization for efficient gene delivery. Macromolecules, **44**, 230–239 (2011). https://doi.org/10.1021/ma102419e

[27] Patil S. S., Torris A., Wadgaonkar P. P.: Healable network polymers bearing flexible poly(lauryl methacrylate) chains *via* thermo-reversible furan-maleimide Diels–Alder reaction. Journal of Polymer Science Part A: Polymer Chemistry, **55**, 2700–2712 (2017). https://doi.org/10.1002/pola.28677

[28] Jakubowski W., Min K., Matyjaszewski K.: Activators regenerated by electron transfer for atom transfer radical polymerization of styrene. Macromolecules, **39**, 39–45 (2006). https://doi.org/10.1021/ma0522716

[29] Wang Y., Lorandi F., Fantin M., Chmielarz P., Isse A. A., Gennaro A., Matyjaszewski K.: Miniemulsion ARGET ATRP *via* interfacial and ion-pair catalysis: From ppm to ppb of residual copper. Macromolecules, **50**, 8417–8425 (2017). https://doi.org/10.1021/acs.macromol.7b01730

[30] Konkolewicz D., Wang Y., Krys P., Zhong M., Isse A. A., Gennaro A., Matyjaszewski K.: SARA ATRP or SET-LRP. End of controversy? Polymer Chemistry, **5**, 4396–4417 (2014). https://doi.org/10.1039/C4PY00149D

[31] Chmielarz P., Król P.: PSt-*b*-PU-*b*-PSt copolymers using tetraphenylethane-urethane macroinitiator through SARA ATRP. Express Polymer Letters, **10**, 302–310 (2016). https://doi.org/10.3144/expresspolymlett.2016.28

[32] Chmielarz P.: Synthesis of inositol-based star polymers through low ppm ATRP methods. Polymers for Advanced Technologies, **28**, 1804–1812 (2017). https://doi.org/10.1002/pat.4065

[33] Magenau A. J. D., Strandwitz N. C., Gennaro A., Matyjaszewski K.: Electrochemically mediated atom transfer radical polymerization. Science, **332**, 81–84 (2011). https://doi.org/10.1126/science.1202357

[34] Lorandi F., Fantin M., Isse A. A., Gennaro A.: Electrochemically mediated atom transfer radical polymerization of *n*-butyl acrylate on non-platinum cathodes. Polymer Chemistry, **7**, 5357–5365 (2016). https://doi.org/10.1039/C6PY01032F

[35] Sun Y., Lathwal S., Wang Y., Fu L., Olszewski M., Fantin M., Enciso A. E., Szczepaniak G., Das S., Matyjaszewski K.: Preparation of well-defined polymers and DNA–polymer bioconjugates *via* small-volume *e*ATRP in the presence of air. ACS Macro Letters, **8**, 603–609 (2019). https://doi.org/10.1021/acsmacrolett.9b00159

[36] Park S., Chmielarz P., Gennaro A., Matyjaszewski K.: Simplified electrochemically mediated atom transfer radical polymerization using a sacrificial anode. Angewandte Chemie International Edition, **54**, 2388–2392 (2015). https://doi.org/10.1002/anie.201410598

[37] Chmielarz P.: Synthesis of α-D-glucose-based star polymers through simplified electrochemically mediated ATRP. Polymer, **102**, 192–198 (2016). https://doi.org/10.1016/j.polymer.2016.09.007

[38] Chmielarz P.: Cellulose-based graft copolymers prepared by simplified electrochemically mediated ATRP. Express Polymer Letters, **11**, 140–151 (2017). https://doi.org/10.3144/expresspolymlett.2017.15

[39] Zaborniak I., Chmielarz P., Wolski K., Grześ G., Isse A. A., Gennaro A., Zapotoczny S., Sobkowiak A.: Tannic acid-inspired star-like macromolecules *via* temporally controlled multi-step potential electrolysis. Macromolecular Chemistry and Physics, **220**, 1900073/1–1900073/8 (2019). https://doi.org/10.1002/macp.201900073

[40] Chmielarz P.: Synthesis of multiarm star block copolymers *via* simplified electrochemically mediated ATRP. Chemical Papers, **71**, 161–170 (2017). https://doi.org/10.1007/s11696-016-0089-0

[41] Matyjaszewski K.: Atom transfer radical polymerization (ATRP): Current status and future perspectives. Macromolecules, **45**, 4015–4039 (2012). https://doi.org/10.1021/Ma3001719

[42] De Bon F., Fantin M., Isse A. A., Gennaro A.: Electrochemically mediated ATRP in ionic liquids: Controlled polymerization of methyl acrylate in [BMIm][OTf]. Polymer Chemistry, **9**, 646–655 (2018). https://doi.org/10.1039/C7PY02134H

[43] De Bon F., Isse A. A., Gennaro A.: Towards scale-up of electrochemically-mediated atom transfer radical polymerization: Use of a stainless-steel reactor as both cathode and reaction vessel. Electrochimica Acta, **304**, 505–512 (2019). https://doi.org/10.1016/j.electacta.2019.03.032

[44] Fantin M., Lorandi F., Isse A. A., Gennaro A.: Sustainable electrochemically-mediated atom transfer radical polymerization with inexpensive non-platinum electrodes. Macromolecular Rapid Communications, **37**, 1318–1322 (2016). https://doi.org/10.1002/marc.201600237

[45] Sumerlin B. S., Neugebauer D., Matyjaszewski K.: Initiation efficiency in the synthesis of molecular brushes by grafting from *via* atom transfer radical polymerization. Macromolecules, **38**, 702–708 (2005). https://doi.org/10.1021/ma048351b

[46] Lu C., Wang C., Yu J., Wang J., Chu F.: Metal-free ATRP 'grafting from' technique for renewable cellulose graft copolymers. Green Chemistry, **21**, 2759–2770 (2019). https://doi.org/10.1039/C9GC00138G

[47] Chmielarz P., Krys P., Wang Z., Wang Y., Matyjaszewski K.: Synthesis of well-defined polymer brushes from silicon wafers *via* surface-initiated *se*ATRP. Macromolecular Chemistry and Physics, **218**, 1700106/1–1700106/13 (2017). https://doi.org/10.1002/macp.201700106

[48] Wang Y., Gong X.: Special oleophobic and hydrophilic surfaces: Approaches, mechanisms, and applications. Journal of Materials Chemistry A, **5**, 3759–3773 (2017). https://doi.org/10.1039/C6TA10474F

[49] Wang Y., Gong X.: Superhydrophobic coatings with periodic ring structured patterns for self-cleaning and oil–water separation. Advanced Materials Interfaces, **4**, 1700190/1–1700190/8 (2017). https://doi.org/10.1002/admi.201700190

[50] Peng J., Zhao X., Wang W., Gong X.: Durable self-cleaning surfaces with superhydrophobic and highly oleophobic properties. Langmuir, **35**, 8404–8412 (2019). https://doi.org/10.1021/acs.langmuir.9b01507

[51] Xia J., Matyjaszewski K.: Controlled/'living' radical polymerization. Atom transfer radical polymerization catalyzed by copper(I) and picolylamine complexes. Macromolecules, **32**, 2434–2437 (1999). https://doi.org/10.1021/Ma981694n

[52] Astanov S., Sharipov M. Z., Faizullaev A. R., Kurtaliev E. N., Nizomov N.: Thermal destruction of riboflavin in different aggregate states. Journal of Applied Spectroscopy, **81**, 37–42 (2014). https://doi.org/10.1007/s10812-014-9883-z

[53] de Farias S. S., Siqueira S. M. C., Cunha A. P., de Souza C. A. G., dos Santos Fontenelle R. O., de Araújo T. G., de Amorim A. F. V., de Menezes J. E. S. A., de Morais S. M., Ricardo N. M. P. S.: Microencapsulation of riboflavin with galactomannan biopolymer and F127: Physico-chemical characterization, antifungal activity and controlled release. Industrial Crops and Products, **118**, 271–281 (2018). https://doi.org/10.1016/j.indcrop.2018.03.039

[54] Neugebauer D., Sumerlin B. S., Matyjaszewski K., Goodhart B., Sheiko S. S.: How dense are cylindrical brushes grafted from a multifunctional macroinitiator? Polymer, **45**, 8173–8179 (2004). https://doi.org/10.1016/j.polymer.2004.09.069

[55] Chmielarz P., Sobkowiak A.: Ultralow ppm *se*ATRP synthesis of PEO-*b*-PBA copolymers. Journal of Polymer Research, **24**, 77/1–77/9 (2017). https://doi.org/10.1007/s10965-017-1235-2

[56] Chmielarz P.: Synthesis of naringin-based polymer brushes *via se*ATRP. Polymers for Advanced Technologies, **29**, 470–480 (2018). https://doi.org/10.1002/pat.4136

[57] Bai L., Zhang L., Cheng Z., Zhu X.: Activators generated by electron transfer for atom transfer radical polymerization: Recent advances in catalyst and polymer chemistry. Polymer Chemistry, **3**, 2685–2697 (2012). https://doi.org/10.1039/C2PY20286G

[58] Wright T. G., Pfukwa H., Pasch H.: Advanced analytical methods for the structure elucidation of polystyrene-*b*-poly(*n*-butyl acrylate) block copolymers prepared by reverse iodine transfer polymerisation. Analytica Chimica Acta, **892**, 183–194 (2015). https://doi.org/10.1016/j.aca.2015.08.005